Published December 16, 2009, doi:10.4049/jimmunol.0901322

Development of Murine Lupus Involves the Combined Genetic Contribution of the *SLAM* and *FcγR* Intervals within the *Nba2* Autoimmune Susceptibility Locus

Trine N. Jørgensen,*[,1,2] Jennifer Alfaro,[†,‡,1] Hilda L. Enriquez,[‡] Chao Jiang,[‡] William M. Loo,[‡] Stephanie Atencio,* Melanie R. Gubbels Bupp,* Christina M. Mailloux,* Troy Metzger,* Shannon Flannery,* Stephen J. Rozzo,* Brian L. Kotzin,*[,3] Mario Rosemblatt,[†,§,¶] María Rosa Bono,[†] and Loren D. Erickson[‡]

Autoantibodies are of central importance in the pathogenesis of Ab-mediated autoimmune disorders. The murine lupus susceptibility locus *Nba2* on chromosome 1 and the syntenic human locus are associated with a loss of immune tolerance that leads to antinuclear Ab production. To identify gene intervals within *Nba2* that control the development of autoantibody-producing B cells and to determine the cellular components through which *Nba2* genes accomplish this, we generated congenic mice expressing various *Nba2* intervals where genes for the *FcγR, SLAM*, and IFN-inducible families are encoded. Analysis of congenic strains demonstrated that the *FcγR* and *SLAM* intervals independently controlled the severity of autoantibody production and renal disease, yet are both required for lupus susceptibility. Deregulated homeostasis of terminally differentiated B cells was found to be controlled by the *FcγR* interval where *FcγRIIb*-mediated apoptosis of germinal center B cells and plasma cells was impaired. Increased numbers of activated plasmacytoid dendritic cells that were distinctly CD19$^+$ and promoted plasma cell differentiation via the proinflammatory cytokines IL-10 and IFNα were linked to the *SLAM* interval. These findings suggest that *SLAM* and *FcγR* intervals act cooperatively to influence the clinical course of disease through supporting the differentiation and survival of autoantibody-producing cells. ***The Journal of Immunology*****, 2010, 184: 000–000.**

Autoantibody-mediated glomerulonephritis (GN) is a major cause of morbidity and mortality in systemic lupus erythematosus (SLE) patients. Considerable evidence from studies using both human patients and mouse models of lupus has indicated that genetic predisposition is a fundamental component in disease susceptibility (1). A common feature among nearly all patients is elevated serum titers of IgG autoantibodies that recognize nuclear Ags (ANA) and contribute to disease by directly mediating tissue damage through the formation of immune complexes (2, 3). This suggests that some susceptibility genes may be broadly involved in disease pathogenesis by predisposing B cells to lose tolerance and inappropriately differentiate to autoantibody-secreting plasma cells (PCs).

The spontaneous lupus-prone (New Zealand Black [NZB] $\times$ New Zealand White [NZW])F_1 and New Zealand Mixed mouse models have been extensively characterized and are considered to replicate human SLE, including clinical features such as a female gender bias and development of severe immune-complex mediated GN. Studies using (NZB $\times$ NZW)F_1 mice and other spontaneous lupus animal models have identified >30 chromosomal loci where genes reside that influence lupus susceptibility or resistance (4). The susceptibility locus (*Sle1*), derived from an NZW-derived interval in the New Zealand Mixed-2410 lupus-prone model, and the locus (*Nba2*), derived from the NZB parental strain, overlap in the telomeric region of chromosome 1, suggesting that some susceptibility genes may be shared among lupus-prone strains. When each locus is expressed on the nonautoimmune C57BL/6 background (B6.*Sle1*; B6.*Nba2*), congenic animals produce elevated levels of ANA IgG, mild splenomegaly, but do not develop severe GN (5–10). Studies by our group have shown that B6.*Nba2* mice resemble NZB mice in their benign autoimmune phenotype. Similarly, when crossed to NZW mice, the female offspring develop fatal kidney disease with similar incidence and kinetics as female (NZB $\times$ NZW)F_1 mice (7, 11).

Included within *Nba2* and *Sle1* are genes encoding members of the *FcγR* family, members of the *SLAM* family of immunomodulatory receptors, and members of the IFN-inducible (*Ifi*) family that can regulate cell proliferation and survival. Sequence analyses have identified polymorphic variants of genes within each of these families in B6, NZB, and NZW mice including *FcγRIIb* (12–15),

*Division of Allergy and Clinical Immunology, University of Colorado Health Sciences Center, Denver, CO 80262; [†]Departmento de Biología, Facultad de Ciencias, Universidad de Chile; [§]Fundación Ciencia para la Vida and Millennium Institute for Fundamental and Applied Biology; [¶]Facultad de Ciencias de la Salud, Universidad Andrés Bello, Santiago, Chile; and [‡]Department of Microbiology, University of Virginia, Charlottesville, VA 22908

[1]T.N.J. and J.A. contributed equally to this work.

[2]Current address: Department of Immunology, Lerner Research Institute, Cleveland Clinic Foundation, Cleveland, OH.

[3]Current address: Amgen, Thousand Oaks, CA.

Received for publication April 27, 2009. Accepted for publication November 10, 2009.

This work is supported by grants from the Lupus Research Institute, Arthritis Foundation, and National Institutes of Health AR052902 to L.D.E., National Institutes of Health 5R01AR37070-19 to B.L.K., Fondecyt 1060253 to M.R., and Fondecyt 1060834 and PFB 16 (Chile) to M.R.B.

Address correspondence and reprint requests to Dr. Loren D. Erickson, Department of Microbiology, University of Virginia, PO Box 800734, Charlottesville, VA 22908. E-mail address: lde9w@virginia.edu

The online version of this article contains supplemental material.

Abbreviations used in this paper: ANA, autoantibody nuclear Ag; cDC, conventional dendritic cell; DC, dendritic cell; GC, germinal center; GN, glomerulonephritis; MHCII, MHC class II; NT, no treatment; NZB, New Zealand Black; NZW, New Zealand White; PC, plasma cell; pDC, plasmacytoid DC; SLE, systemic lupus erythematosus.

the *SLAM/CD2* gene cluster (16, 17), and *Ifi202* (7). Because of the complicated pattern of disease-associated genes in the *Nba2* locus, it is unknown whether the *FcγR*, *SLAM*, and *Ifi* gene clusters contribute to the autoimmune phenotype as a group or as individual gene clusters.

In this study, we directly evaluated the role of *Nba2*-derived *FcγR*, *SLAM*, and *Ifi* gene clusters in autoantibody production by creating congenic mice that vary in expression of these three intervals. Analysis of congenic strains demonstrated that the severity of ANA and renal disease are linked with the *FcγR* and *SLAM* gene clusters with little involvement from the *Ifi* interval. The most severe autoimmune phenotype occurs in mice carrying both *FcγR* and *SLAM* clusters from the parental B6.*Nba2* strain. Analyses of immune cell function among the congenic strains revealed that spleen dendritic cells (DCs), including an expanded population of $CD19^+$ plasmacytoid DCs (pDCs), inappropriately supported PC differentiation in a cytokine-dependent manner that was linked to the *SLAM* gene cluster. Reduced expression of and apoptosis mediated by *FcγRIIb* were found in B cells that was directly controlled by the *FcγR* gene interval. Thus, although the *FcγR* and *SLAM* gene clusters independently control different immune pathways in murine lupus, together, they contribute to lupus susceptibility by cooperatively controlling autoantibody production.

Materials and Methods

Mice and evaluation of autoimmune phenotype

Congenic B6.*Nba2*-ABC mice were previously described (7). Congenic strains expressing smaller intervals of the initial *Nba2* lupus susceptibility locus were generated by backcrossing 10 generations with B6 mice. These are referred to as B6.*Nba2*-A (154.7-174.5Mb), B6.*Nba2*-A′B (169.1-175.9Mb), B6.*Nba2*-B (172.8-175.9Mb), B6.*Nba2*-BC (172.8-194.1Mb), and B6.*Nba2*-C (174.5-194.1Mb). Genotyping was performed using a panel of microsatellite markers distributed across the distal chromosome 1 (Supplemental Table I). The positions of markers and various candidate genes with respect to the centromere are given in accordance with the Mouse Chromosome Committee Reports (obtainable at the Mouse Genome Database at www.informatics.jax.org). The PCR products of all D1Mit markers, *Crp* and *FcγRIIb* were separated on 10% polyacrylamide gels, whereas real-time PCR reactions for *Ifi202* were run on a BioRad iCycler IQ (Bio-Rad, Hercules, CA) to determine whether the marker was of B6 or NZB origin. B6, NZW, NZB, and $(NZB \times NZW)F_1$ female mice were purchased from The Jackson Laboratory (Bar Harbor, ME). All mice used in these studies were maintained in the specific pathogen-free animal facilities at the University of Colorado Health Sciences Center (Denver, CO) or at the University of Virginia (Charlottesville, VA). All animal procedures were conducted in compliance with the National Institutes of Health guidelines and are approved by the Institutional Animal Care and Use Committee of each institution.

All experiments were performed with 4- to 12-mo-old female mice unless indicated and were tested for proteinuria on a monthly basis as previously described (6, 18). Mice were terminated at 12 mo of age or if designated as positive for kidney disease by severe proteinuria (i.e., ≥100 mg/dl protein) in the urine on two consecutive measurements, which has been previously established to predict mortality from renal failure (6, 18).

Serum autoantibody IgG levels to chromatin, total histones, and dsDNA were determined by ELISA as previously described (18). Briefly, serum samples were diluted 1:300 and applied to Ag-coated (chromatin, total histones, or a biotinylated dsDNA-streptavidin complex) 96-well plates in duplicates. OD values were converted to units per milliliter by comparison with a standard curve obtained using mAbs toward DNA or histones. Animals were considered positive if they reached levels higher than the mean ± 2 SD of age-matched control B6 mice.

Detection of Ifi202 *and VDJ rearrangement by RT-PCR*

Total RNA was isolated from freshly isolated spleen cells using the RNeasy System (Qiagen,Valencia, CA) and was treated with DNase I before cDNA synthesis. *Ifi202* transcripts were analyzed by real-time RT-PCR using the SYBR Green PCR Core Kit (Applied Biosystems, Foster City, CA) on an iCycler iQ instrument (Bio-Rad) and normalized to the transcript levels of the housekeeping gene *Actin*. Primer and probe sequences are provided in Supplemental Table I. Units of *Ifi202* gene expression was calculated based on the average level of *Ifi202* RNA in spleen cells from 16-wk-old NZB females (set at 1 unit). Equal amounts of protein were processed for immunoblotting using antiserum to *Ifi202* (S-19; Santa Cruz Biotechnology, Santa Cruz, CA). DNA samples from sort-purified spleen B cells, conventional DC (cDC), $CD19^-$ pDC, and $CD19^+$ pDC subsets were analyzed for VDJ rearrangement by RT-PCR as previously described (19).

Flow cytometry

Cells were washed and resuspended in 5% bovine calf serum in balanced salt solution and stained with a mixture of mAbs, as noted, for the detection of multiple cell surface and intracellular Ags. Purified rat IgG was used as an isotype control. Nonspecific staining was reduced by the addition of rat serum Ig. Stained cells were incubated for 30 min at 4°C, followed by washing in balanced salt solution. Incubation with streptavidin-PE-cyanin 5.5 was performed for an additional 30 min at 4°C, followed by washing. DAPI was added to cells at a concentration of 5 μM/ml to discriminate live versus dead cells. After surface staining, samples requiring intracellular staining were labeled for caspase-3 using the Cytofix/Cytoperm reagent (BD Biosciences, San Jose, CA) according to the manufacturer's instructions. Cell acquisition was performed with a DakoCytomation CyAN ADP LX (Carpinteria, CA), where a minimum of 100,000 events was collected. Spectral overlap compensation and data analysis were performed using FlowJo software (Tree Star, Ashland, OR). Profiles are presented as 5% probability contours including outliers with gating based on fluorescence-minus-one and isotype controls.

FcγRIIb *cross-linking*

Single-cell suspensions were prepared from spleens of mice that were immunized with the T cell-dependent NP-KLH Ag for 7 d to generate PCs and germinal center (GC) B cells. Cells were depleted of RBC by ammonium chloride-Tris lysis, washed in RPMI 1640, and cultured 4 h in 96-well plates precoated with 10 μg/ml of rat IgG $F(ab')_2$ or anti-FcγRII/III (2.4G2) mAb ± 20 μM of the caspase-3 inhibitor benzylocarbonyl-Val-Ala-Asp(OMe)-fluoromethylketone (ZVAD; MP Biochemicals, Solon, OH). At the end of the culture, cells were harvested and analyzed by flow cytometry to measure apoptosis by intracellular expression of the cleaved active form of caspase-3 from GC B Cells ($B220^+GL7^+$) and PCs ($B220^{low/-}CD138^+$). Cells cultured in 10 μM DMSO served as a positive control for apoptosis.

Isolation of splenic DCs

Spleens were incubated for 45 min at 37°C in complete RPMI 1640 supplemented with 5% FBS and 1mg/ml collagenase D (Roche, Indianapolis, IN), followed by homogenization. Single-cell suspensions were washed in RPMI 1640 and depleted of RBC by ammonium chloride-Tris lysis. Total $CD11c^+$ DCs were positively selected using anti-CD11c MACS (clone N418; Miltenyi Biotec, Auburn, CA) after the manufacture's protocol. As indicated, some experiments used electronically sort-purified DCs using a FACSVantage SE TurboSort to produce cDC ($CD11c^{high}B220^-CD19^-$), $CD19^-$ pDC ($CD11c^{int}B220^+CD19^-$), and $CD19^+$ pDC ($CD11c^{int}B220^+CD19^+$) populations of >98% purity.

DC morphology by cytospin

Sort-purified B cells, cDCs, and pDCs were cytospun onto glass slides (5 min at 230*g*) and fixed in methanol for 5 min at room temperature. Slides were washed and stained with Giemsa (Sigma-Aldrich, St. Louis, MO), followed by digital photography. All images were taken at original magnification ×40.

In vitro TLR stimulation

DCs (2×10^5) were cultured in 96-well plates for 24 h in complete RPMI 1640 supplemented with 10% FBS alone or containing 10 μg/ml CpG (ODN 1826; InvivoGen, San Diego, CA), 100 ng/ml LPS (Sigma-Aldrich), or 10μg/ml imiquimod (R837) (InvivoGen). At the end of the culture, supernatants were collected and tested for cytokines by ELISA.

For DC and B cell coculture experiments, electronically sort-purified pDCs and B cells from spleen were cultured separately (1×10^5/well) or together in 96-well round bottom plates for 3 d in complete RPMI 1640 supplemented with 10% FBS alone, 10 μg/ml CpG, or 10 μg/ml nonstimulatory GpC control oligonucleotide for ODN1826 (InvivoGen). Neutralizing mAbs specific for IL-6 (clone MP5-20F3; eBiosciences, San Diego, CA), IL-10 (clone JES52A5; eBiosciences), IL-12 (clone C17.8; eBiosciences), and IFNα (clone RMMA-1; PBL InterferonSource, Piscataway, NJ) were present at 5 μg/ml throughout the culture as indicated. Irrelevant rat IgG served as a nonspecific mAb control. At the end of the culture, cells were harvested and the number of PCs determined by ELISPOT.

Measurement of cytokines by ELISA

Murine IL-6, IL-10, and IL-12/p70 were measured using the Duo Set kit (R&D Systems, Minneapolis, MN) according to the manufacturer's instructions. IFNα was determined by sandwich ELISA using the rat anti-mouse IFNα RMMA-1 mAb for cytokine capture and the rabbit anti-mouse IFNα polyclonal Ab for cytokine detection (PBL InterferonSource). HRP-conjugated AffiniPure $F(ab')_2$ fragment donkey anti-rabbit IgG (H+L) was used as a secondary Ab (Jackson ImmunoResearch Laboratories, West Grove, PA). Assays were developed using tetramethylbenzidine substrate (BD Biosciences).

Measurement PCs by ELISPOT

IgM- and IgG-secreting PCs were quantified by ELISPOT assay as previously described (20). Briefly, harvested cells from DC and B cell cocultures were resuspended in complete RPMI 1640 and incubated for 6 h on multiscreen 96-well plates (Millipore, Bedford, MA) precoated with unlabeled anti-mouse IgM and IgG. Serial dilutions of cells were made with an initial cell concentration of 20,000/well. After incubation, plates were washed in 0.05% Tween 20 and incubated with secondary HRP-conjugated Abs to detect mouse IgM and IgG (Southern Biotechnology Associates, Birmingham, AL). ELISPOT assays were developed by FAST 5-bromo-4-chlor-3-indolyl phosphate/NBT chromogen substrate (Sigma-Aldrich). The number of Ig-secreting spots was quantified by direct visual counting using a dual-axis light dissecting microscope.

Statistical analyses

All statistical analyses on autoantibody levels between study groups were performed using the nonparametric, Mann-Whitney *U* test. A curve comparison test was used to determine statistical differences in the development of proteinuria between study groups. Unpaired comparisons between samples from congenic strains and control mice were analyzed by the Student *t* test for cell frequencies, mean fluorescence intensities, and cytokine secretion. p Values ≤ 0.05 were considered significant and are denoted in figure legends.

Online supplemental material

The PCR primer sequences used for genotyping are shown in Supplemental Table I. A summary of ANA IgG production in 7-mo-old congenic strains and F_1 progeny of crosses with NZW mice is shown in Supplemental Table II. A comparison of serum ANA IgG and cytokine (IFNα, IL-6, IL-10, and IL-12) levels in 4- and 7-mo-old animals is shown in Supplemental Fig. 1. *Ifi203* transcript expression levels in splenocytes from congenic strains are shown in Supplemental Fig. 2. *FcγRIIb* transcript expression levels in purified splenic $CD138^+$ PCs from congenic strains are shown in Supplemental Fig. 3. Surface protein expression levels of activation molecules and *SLAM* receptors on DC subsets are shown in Supplemental Fig. 4. Transcript expression levels of the *SLAM* family members CD48, CD84, CD150, CD229, Ly108.1, and Ly108.2 in purified pDCs are shown in Supplemental Fig. 5. IL-10 production by TLR-activated DCs from control and congenic strains is shown in Supplemental Fig. 6.

Results

*Generation of B6.*Nba2 *congenic strains that express different regions of the* Nba2 *locus and the development of an autoimmune phenotype*

To determine the contribution of individual gene clusters within *Nba2* in the development of lupus traits, we repeatedly backcrossed the parental B6.*Nba2* strain to the nonautoimmune B6 strain and genotyped progeny for the inheritance of truncated *Nba2* intervals by PCR (Supplemental Table I). Siblings were then intercrossed to generate subcongenic strains homozygous for the interval. Five strains were selected for further study based on inheritance of intervals where genes for the *FcγR*, *SLAM*, and *Ifi* families are encoded (Fig. 1). To more easily refer to these strains, we have labeled them according to inheritance of the proximal (A), central (B), and distal (C) regions of *Nba2*. The parental B6.*Nba2* strain is referred to as B6.*Nba2*-ABC.

Female, 7-mo-old congenic strains were followed for the development of ANA IgG by measuring Ab titers in sera by ELISA (Fig. 2; summarized in Supplemental Table II). Results demonstrated that IgG levels specific for chromatin, histones, and dsDNA were higher in B6.*Nba2*-ABC congenic animals compared with the B6.*Nba2*-B strain that carries only the *Nba2*-derived *SLAM* interval, which produced modest levels of antichromatin IgG (1.06 ± 0.30 U/ml, $p < 0.01$), but insignificant levels of histone- and dsDNA-specific IgG comparable to B6 control animals (Fig. 2*A*). The B6.*Nba2*-BC strain that carries the *Nba2*-derived *SLAM* and *Ifi* intervals, as well as the distal region of *Nba2,* produced similar ANA levels to B6.*Nba2*-B mice. In contrast, B6.*Nba2*-C mice that differ from B6.*Nba2*-BC mice only in inheritance of the *SLAM* interval from the B6 genome produced significantly reduced levels of antichromatin IgG (0.22 ± 0.07 U/ml, $p < 0.05$). These data suggest that the distal region of *Nba2*, including the *Ifi* interval, is dispensable for ANA production. To further test this hypothesis, we compared serum ANA IgG levels in B6.*Nba2*-A′B and B6.*Nba2*-A congenic strains that both express the *Nba2*-derived *FcγR* interval but differ in the expression of the *SLAM* gene cluster. Results demonstrated that B6.*Nba2*-A mice produced modest levels of antichromatin IgG (1.54 ± 0.43 U/ml, $p < 0.01$), which was comparable to levels observed in B6.*Nba2*-B animals and suggests that gene(s) within the proximal region of *Nba2* can also contribute to ANA production. Interestingly, the B6.*Nba2*-A′B strain that expresses only the *FcγR* and *SLAM* intervals from *Nba2* produced significantly elevated levels of IgG to all three nuclear Ags and essentially reproduced ANA levels measured in the parental B6.*Nba2*-ABC strain (Fig. 2*A*). Measurement of serum ANA IgG in 4-mo-old congenic strains demonstrated low ANA levels compared with their 7-mo-old counterparts (Supplemental Fig. 1), indicating that elevated autoantibody production is age-dependent. Analysis of lupus-associated cytokine levels in serum demonstrated low amounts of IFNα and IL-6, and little to none of IL-10 and IL-12 among 4- and 7-mo-old strains (Supplemental Fig. 1), suggesting that increased ANA levels in older mice was not the result of high-circulating cytokine levels that often correlate with SLE-like manifestations. These data indicate that combined expression of the *FcγR* and *SLAM* gene clusters from *Nba2* is sufficient for controlling autoantibody production.

To further test the contribution of *Nba2* gene intervals in ANA production and tissue damage, congenic strains were crossed with NZW mice and female 7-mo-old F_1 mice were followed for ANA IgG (Fig. 2*B*) and kidney failure (Fig. 2*C*). Results demonstrated that (B6.*Nba2*-ABC × NZW)F_1 mice produced high levels of ANA IgG and >90% of animals developed kidney disease by 1 y of age, which is consistent with previous studies by our group (7, 21). In contrast, control (B6 × NZW)F_1 mice produced insignificant levels of autoantibodies (Fig. 2*B*), and do not develop proteinuria (7). Analyses of the F_1 progeny from each subcongenic strain crossed with NZW revealed that the B6.*Nba2*-A′B strain reproduced the autoimmune phenotype of B6.*Nba2*-ABC mice. Although B6.*Nba2*-B and B6.*Nba2*-BC mice produced only modest levels of antichromatin IgG (Fig. 2*A*), high levels of IgG specific for all three nuclear Ags were produced when crossed to the NZW strain, and by 1 y of age 65% of female F_1 mice had severe proteinuria. Finally, nominal amounts of ANA IgG were measured in F_1 progeny of B6.*Nba2*-A and B6.*Nba2*-C strains and correlated with proteinuria occurring in <25% and 0% of F_1 animals, respectively. These results confirm that both *FcγR* and *SLAM* intervals, but not the *Ifi202* interval of the *Nba2* locus, mediate ANA production and the development of lupus nephritis.

Additional PCR and Western blot analyses showed that spleen cells of congenic BC and C strains expressed increased *Ifi202* transcript and protein levels, whereas congenic A and A′B strains expressed low levels of *Ifi202* (Fig. 3). These data confirm that increased levels of this transcript are related specifically to the allelic derivation of *Ifi202*. B6.*Nba2*-ABC and B6 mice served as positive and negative controls for *Ifi202* expression as previously reported (7, 22). These data provide additional evidence that increased *Ifi202* expression is not sufficient for ANA production. Expression levels of *Ifi203*, previously demonstrated to be reciprocally low in B6.

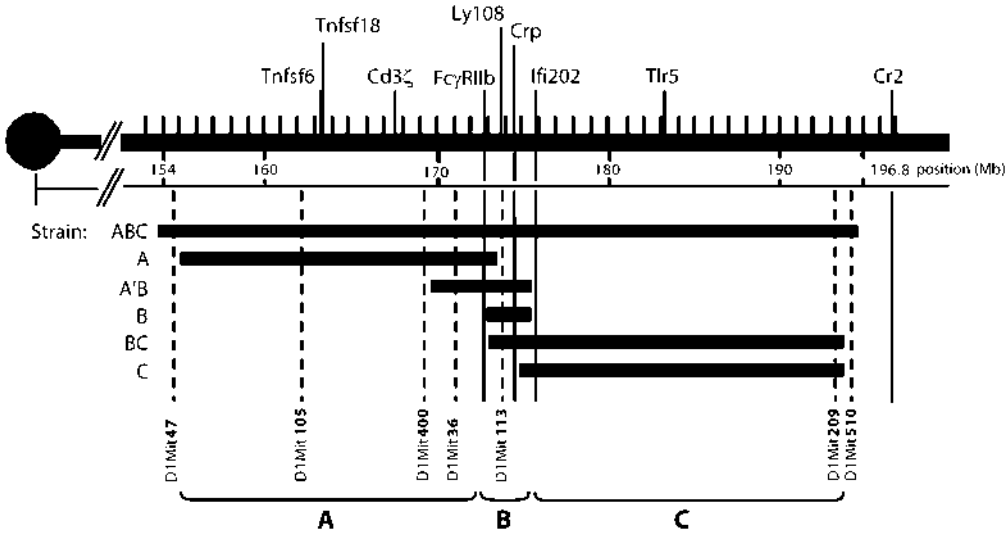

FIGURE 1. Map of telomeric chromosome 1 encoding *Nba2* and the congenic strains generated to express various intervals. Distal chromosome 1 with the positions of known immune regulatory genes is shown. Dashed lines show microsatellite markers used to determine B6 or NZB origin. Congenic strains are identified according to inheritance of proximal (*A*), central (*B*), and distal (*C*) regions that encompass the *Nba2* locus.

Nba2-ABC mice (7), were reduced in congenic strains harboring the NZB-derived *Ifi* interval, providing further confirmation (Supplemental Fig. 2).

Inheritance of the NZB FcγR *interval from* Nba2 *results in decreased expression of the FcγRIIb inhibitory receptor during terminal B cell differentiation and is associated with impaired apoptosis*

Signaling via the inhibitory FcγRIIb, which is the only Fcγ receptor expressed on murine B cells (23), can modify B cell responses and mediate apoptosis (24–26). Polymorphisms in the NZB *FcγRIIb* promoter have been identified within *Nba2* that can result in the failure to upregulate FcγRIIb expression on GC B cells and PCs of NZB mice (13–15). Thus, impaired FcγRIIb expression could mediate B cell hyperactivity and survival in congenic B6.*Nba2* strains. We therefore determined by flow cytometric analysis whether FcγRIIb membrane expression could be upregulated as B cells differentiated to GC B cells and PCs in vivo. Splenocytes of mice that were immunized for 7 d with the T cell-dependent Ag, NP-KLH, were prepared and labeled with fluorescent-conjugated mAbs specific for the B cell marker B220, the GC marker GL7 (27), the PC marker CD138 (28), and FcγRII/RIII. Because FcγRIII is not expressed on murine B cells, this identifies B cells expressing FcγRIIb alone. Results demonstrated that GC B cells and PCs from spleens of control B6 mice express increased FcγRIIb levels compared with mature B cells (Fig. 4*A*). This pattern of expression was also found on GC B cells and PCs from congenic B, BC, and C strains that all carry the control B6-derived *FcγR* interval. In contrast, FcγRIIb failed to be upregulated on both GC B cells and PCs from B6.*Nba2*-ABC mice and on PCs alone from congenic A and A′B strains. We confirmed reduced expression of *FcγRIIb* mRNA transcript levels in PCs from congenic ABC mice, and not from B and C strains, consistent with protein expression (Supplemental Fig. 3) and suggesting that impaired upregulation of membrane FcγRIIb expression on terminally differentiated B cells is controlled at the transcriptional level. Interestingly, a subset of GC B cells from congenic A and A′B mice upregulated FcγRIIb expression. These findings suggest that genes within the C region of *Nba2* such as the *Ifi* family may contribute to impaired FcγRIIb expression because GC B cells from B6.*Nba2*-ABC animals completely failed to upregulate FcγRIIb.

Analysis of the absolute cell numbers from the various strains revealed an increase in the overall numbers of splenic B cells among the congenic strains compared with control B6 mice (Fig. 4*B*). Thus, inheritance of the A, B, or C region of *Nba2* influences the frequency of spleen B cells. Enumeration of total GC B cells within spleens of congenic strains maps this phenotype to the A region because we found significantly increased numbers of GC B cells in congenic ABC, A, and A′B animals compared with B6 mice or congenic lines without the NZB-derived A region ($p < 0.05$). Finally, total PC numbers were highest in congenic ABC and A′B strains ($p < 0.05$), suggesting that combined expression of the distal A region and B region within *Nba2* control PC survival.

We next determined whether differential FcγRIIb expression among the congenic strains controlled apoptosis. Purified spleen B cells were stimulated with culture grade anti-FcγRII/III Ab or IgG $(Fab')_2$ in vitro and analyzed by flow cytometry for the intracellular expression of the cleaved, active form of caspase-3 as an indicator of apoptosis. Results demonstrated that GC B cells and PCs of congenic ABC, A, and A′B mice did not undergo apoptosis in response to FcγRIIb cross-linking compared with cells from control mice and congenic B, BC, and C strains (Fig. 4*C*). Apoptosis in these latter strains was specific for FcγRIIb because GC B cells and PCs failed to undergo apoptosis when cultured with IgG $(Fab')_2$. Confirmation of FcγRIIb-mediated apoptosis was further provided by analysis of cells from cultures that contained the caspase-3 inhibitor ZVAD. Staining for caspase-3 from all B cells in response to DMSO exposure served as positive controls for all strains. Together, these results indicate that the *FcγR* interval within *Nba2* impairs FcγRIIb expression and function on terminally differentiating B cells, suggesting that this interval influences survival.

Inheritance of the SLAM *interval within* Nba2 *is associated with heightened numbers of spleen DC subsets that have an altered phenotype*

DCs initiate and regulate humoral immunity by controlling T and B lymphocyte activation through expression of membrane-anchored costimulatory proteins as well as secreted factors (29, 30). Thus, it is believed that DCs play a critical role in maintaining tolerance during Ag recognition by lymphocytes. We therefore determined the frequency of the two main DC subsets, cDC and pDC, in spleens of 4-mo-old female mice based on the level of CD11c and

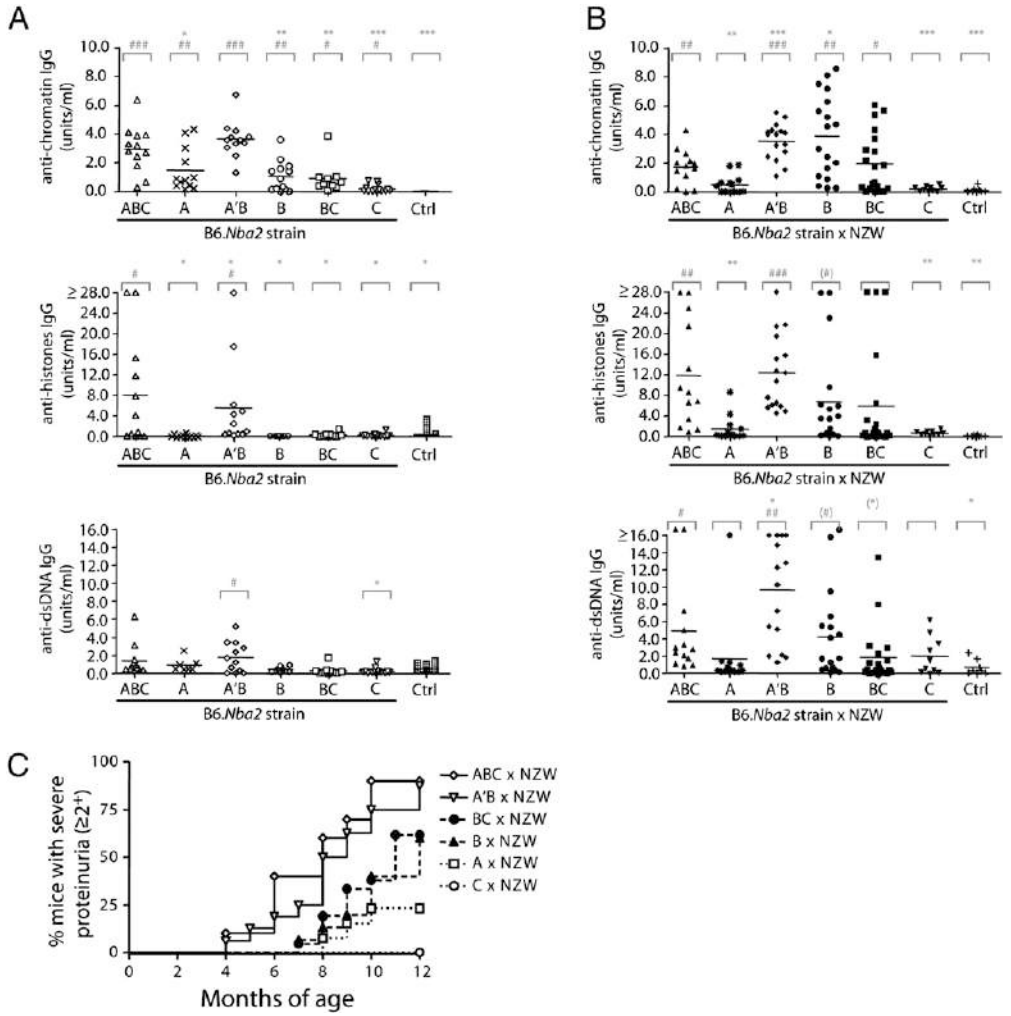

FIGURE 2. *Fcγ R* and *SLAM* gene clusters within *Nba2* are sufficient for autoantibody production and renal failure. Sera from female, 7-mo-old congenic strains (*A*) and F_1 mice from congenic strains crossed with NZW (*B*) was analyzed for IgG autoantibodies to chromatin, total histones, and dsDNA by ELISA. Statistical differences between congenic strains and control mice are indicated as #$p < 0.05$, ##$p < 0.01$, and ###$p < 0.001$. Statistical differences between each group and B6.*Nba2*-ABC or (ABC × NZW)F_1 mice are indicated as *$p < 0.05$, **$p < 0.01$, and ***$p < 0.001$. *C*, Proteinuria levels were determined in female F_1 mice on a monthly basis for 12 mo. Data are shown as the percentage of mice within each group whose proteinuria levels were ≥100 mg/dl protein. Each group consisted of at least 13 mice. The difference in frequency of disease in the (B6.*Nba2*-ABC × NZW)F_1 and (B6.*Nba2*-A′B × NZW)F_1 mice compared with other groups by 8 mo of age was significant, $p < 0.001$.

B220 expression (Fig. 5*A*). The percentages of cDC and pDC within total spleen cells were used to quantify absolute numbers for each strain. Results demonstrated that total numbers of pDCs were significantly increased in spleens of congenic ABC, A′B, and B mice compared with control animals. Although modest splenomegaly was observed in the congenic ABC strain, we found no statistically significant differences in the total cellularity of spleens between the subcongenic strains and control mice. In contrast, an increase in the percentage values of total pDCs was determined from ABC (38%), A′B (34%), and B (29%) strains compared with B6 controls (13%), suggesting that increased numbers of total pDCs is not attributed to a dramatic increase in overall cellularity. Absolute numbers of pDCs were also increased in congenic A and C strains compared with controls, but overall were lower than other strains; these differences were not statistically significant. Total numbers of splenic cDCs among congenic lines were generally higher than in control mice, but these differences were much smaller compared with numbers of pDCs and were not statistically significant. These data suggest that expression of the *SLAM* interval (B6.*Nba2*-ABC, -A′B, and -B strains) controls the development and/or life span of pDCs.

We have previously demonstrated that type I IFN (IFNαβ) signaling is involved in the spontaneous development of renal disease in (B6.*Nba2*-ABC × NZW)F_1 mice (21, 31). Within healthy mice, it has been demonstrated that the highest amount of IFNα is produced by a minor subset of pDCs that expresses the marker CD19 (32, 33). We therefore determined the steady-state frequencies of $CD19^{--}$ and $CD19^+$ pDCs in spleens of 2- and 4-mo-old mice by flow cytometry (Fig. 5*B*). Results demonstrated that $CD19^+$ pDCs represented a low percentage of overall pDCs in B6 control mice regardless of age. In contrast, B6.*Nba2*-ABC mice showed an increased frequency of $CD19^+$ pDCs in an age-dependent manner with $CD19^+$ pDCs representing ~3% and 25% of total pDCs in 2- and 4-mo-old mice, respectively. Absolute numbers of $CD19^-$ pDCs were similar in all strains tested. In contrast, strains expressing the *Nba2*-derived *SLAM* interval (ABC, A′B, and B mice) yielded a statistically significant higher number of $CD19^+$ pDCs (Fig. 5*B*). Siglec-H receptor expression has previously been demonstrated to be restricted to type I IFN-producing pDCs (34, 35). We confirmed that essentially no cDCs ($CD11c^{high}B220^-PDCA1^-$) expressed Siglec-H (Fig. 5*C*). However, both $CD19^-$ and $CD19^+$ pDCs ($CD11c^{int}B220^+PDCA1^+$)

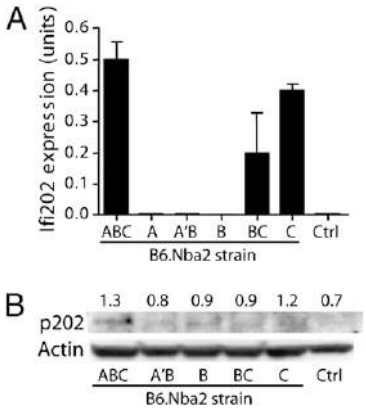

FIGURE 3. Expression levels of *Ifi202* correspond with the *Nba2* genotype of congenic strains. *A*, Real-time PCR analysis of *Ifi202* expression in spleen cells from 4-mo-old congenic strains and B6 control mice. Results are expressed as the mean ± SEM from six mice. *B*, Extracts prepared from individual age-matched female mice were analyzed by immunoblotting using Abs specific to the indicated proteins. Densitometry values of protein expression relative to β-actin are shown. Data are representative of two experiments.

expressing Siglec-H were increased in frequency within congenic ABC, A′B, and B strains compared with control mice. Although a greater percentage of $CD19^-$ pDCs expressed Siglec-H relative to $CD19^+$ pDCs, quantified numbers of total cells shown in Fig. 5*B* indicated that the majority of pDCs were $CD19^+$. These findings indicate that the central region of *Nba2* inappropriately controls the homeostasis of $CD19^+$ pDCs in an age-dependent manner and promotes the expression of Siglec-H on both $CD19^-$ and $CD19^+$ pDCs, suggesting that these cells may produce IFNα.

Previous studies have demonstrated that *Nba2* does not influence the percentage of marginal zone B cells and B1 B cells in spleen (36). However, because of the dramatic and novel increase in $CD19^+$ pDCs within *Nba2* congenic strains, we performed three additional analyses to confirm that this population was not the result of contaminating B cells. First, we electronically sort-purified B cells, cDCs, $CD19^-$ pDCs, and $CD19^+$ pDCs from spleens of B6.*Nba2*-ABC mice and analyzed Ig gene rearrangement by PCR using a previously established strategy (19). This approach amplifies DNA corresponding to sequences that are lost on D-J rearrangement (5′ J_H1) and that are lost on V to D-J rearrangement (5′ $D_{FL16.1}$). Thus, amplification of J_H1 and $D_{FL16.1}$ transcripts will be lost in bona fide B cells. Because it has been demonstrated that low levels of D-J rearrangement can occur in splenic pDCs but not cDCs using other PCR-based strategies (37–39), we chose this strategy as a more unambiguous method to determine whether $CD19^+$ pDCs were comprised of B-lineage cells. This measure of Ig gene rearrangement clearly distinguished our cDC, $CD19^-$ pDC, and $CD19^+$ pDC populations from B cells (Fig. 6*A*). Second, we morphologically assessed cytospins of sort-purified DCs and B cells by Giemsa staining (Fig. 6*B*). Results demonstrated that $CD19^+$ pDCs had the classical appearance of DCs, including large distinct nuclei, a very small cytoplasm, and dendrite formation (arrows) compared with B cells (40). Finally, we used multiparameter flow cytometry to define cDC and pDC subsets on the basis of cell surface marker expression (41, 42). In this study, we restricted our analyses to congenic ABC, A′B, and B strains as well as control mice because increased pDC numbers were statistically associated with these strains. Results

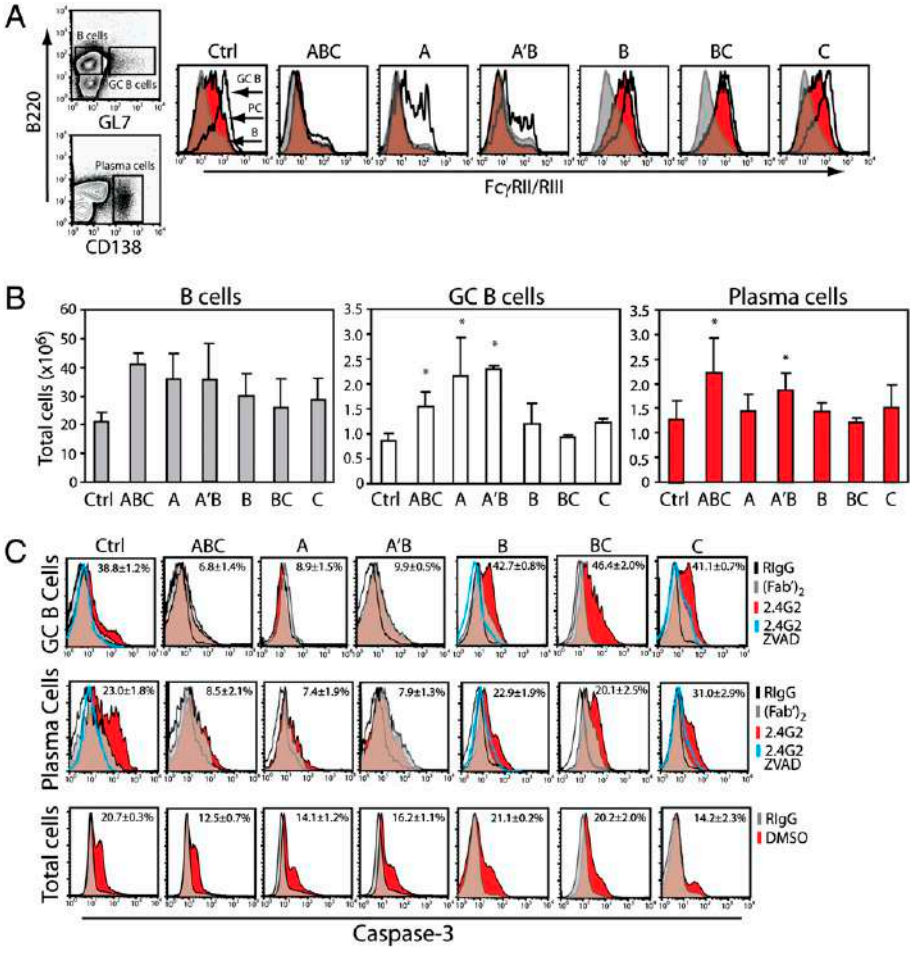

FIGURE 4. Reduced levels of FcγRIIb expression on PCs and GC B cells are associated with *Nba2* genotype. Spleen cells were prepared from 4-mo-old female mice immunized with 100 μg NP-KLH Ag for 7 d. *A*, The levels of FcγRIIb membrane expression on $DAPI^-B220^+GL7^+$ gated GC B cells (open black histograms), $DAPI^-B220^{low/-}CD138^+$ gated PCs (solid red histograms), and $DAPI^-B220^+GL7^-$ gated B cells (solid gray histograms) were determined by flow cytometry. *B*, Total numbers were quantified for the indicated cell populations from immune animals shown in *A*. Data shown are expressed as the mean ± SEM for six mice per group. Statistical differences between congenic strains and B6 control mice are indicated as $*p < 0.05$. *C*, T cell-depleted spleen cells were cultured 4 h with plate-bound rat IgG $(Fab')_2$ (gray histograms), anti-FcγRIIb (2.4G2; red histograms) alone, or with the caspase-3 inhibitor ZVAD (blue histograms). Apoptosis was determined by intracellular caspase-3 staining of GC B cells and PCs. Numbers represent the percentage of apoptotic cells. Open black histograms represent isotype-matched control staining. Cells cultured 4 h in the presence of 10 μM DMSO were stained for intracellular caspase-3 (*bottom row*; red histograms) as a positive control for apoptosis. Solid gray histograms represent isotype-matched Ab staining.

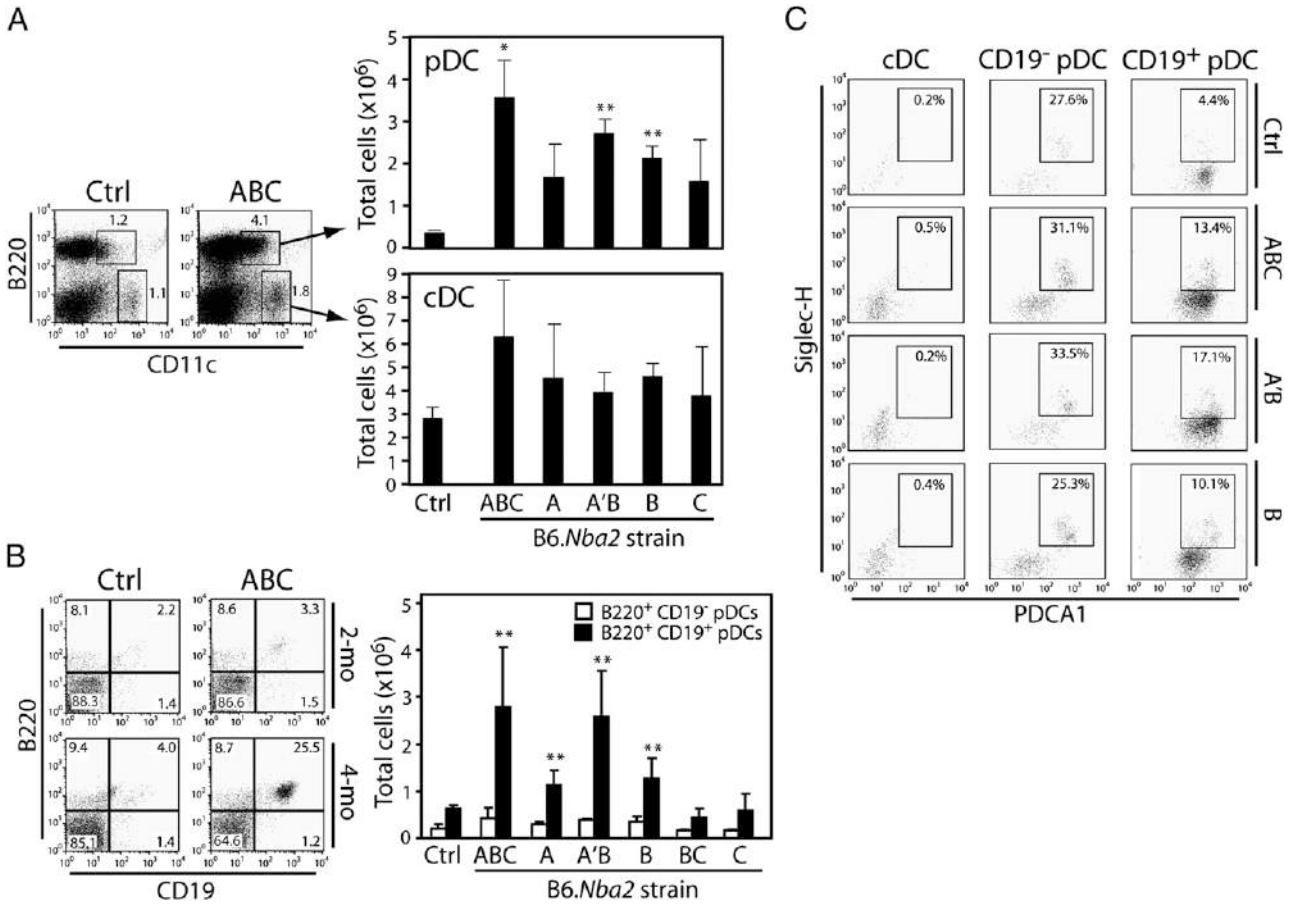

FIGURE 5. *Nba2* controls the frequency and subset distribution of pDCs in an age-dependent manner. *A*, Total numbers of pDCs ($DAPI^-B220^+CD11c^{int}$) and cDCs ($DAPI^-B220^-CD11c^{high}$) from spleens of 4-mo-old congenic strains were determined by flow cytometry. Data are expressed as the mean ± SEM for nine mice per group. Statistical differences between congenic strains and B6 control mice are denoted by $*p < 0.05$ and $**p < 0.01$. *B*, Total $B220^+CD11c^{int}$ gated pDCs from spleens of 2- and 4-mo-old congenic strains were further segregated into $CD19^-$ and $CD19^+$ pDC subsets and absolute numbers were determined. Statistical differences between congenic strains and control mice are indicated as $**p < 0.01$. *C*, The expression of Siglec-H and PDCA1 was determined on cDCs, $CD19^-$ pDCs, and $CD19^+$ gated pDCs from spleens of the indicated strains.

demonstrated that cDCs from all strains exhibited a phenotype consistent with murine cDCs, including high levels of MHC class II (MHCII) expression, negative expression of the pDC marker PDCA1, little CD4 staining, and a bimodal distribution of CD8α that segregates cDCs into lymphoid ($CD8\alpha^{high}$) and myeloid ($CD8\alpha^-$) DC subsets. $CD19^-$ pDCs from control and B6.*Nba2*-B mice exhibited a phenotype consistent with murine pDCs, including lower levels of MHCII expression, positive staining for PDCA1, and variable levels of CD4 and CD8α staining. $CD19^-$ pDCs from congenic ABC and A′B strains demonstrated an equivalent staining profile with the exception of increased MHCII expression. Interestingly, $CD19^+$ pDCs from all strains unimodally expressed high levels of PDCA1, no CD4 staining, and variable but increased levels of CD8α expression compared with their $CD19^-$ pDC counterparts. In contrast to $CD19^-$ pDCs, $CD19^+$ pDCs from all strains expressed higher levels of MHCII with statistically significant greater expression of MHCII on $CD19^+$ pDCs from the ABC and A′B congenic strains compared with controls (Fig. 6*C*). None of the DC subsets stained positive for F4/80 and NK1.1 (Supplementl Fig. 4), indicating that macrophages and the more recently identified $NK1.1^+$ DC subset were not present (40, 43). These data suggest that $CD19^+$ pDCs are bona fide pDCs based on marker expression, yet are distinct from $CD19^-$ pDCs with regard to steady-state MHCII expression levels. Furthermore, increased expression of MHCII on both $CD19^-$ and $CD19^+$ pDCs of ABC and A′B congenic strains suggests that the *Fcγ R* and *SLAM* intervals of *Nba2* influence the activation state of pDCs.

Steady-state expression levels of the costimulatory molecules CD40, CD80, and CD86 were also examined to determine whether pDCs exhibited an altered activation phenotype. Results demonstrated that although $CD19^+$ pDCs overall expressed higher amounts of CD40 compared with their $CD19^-$ pDCs counterparts, both $CD19^-$ and $CD19^+$ pDCs from ABC and A′B congenic strains expressed significantly higher levels of CD40 (Fig. 6*C*). No significant differences in CD80 expression were measured among the strains albeit $CD19^+$ pDCs generally expressed higher levels of CD80 compared with $CD19^-$ pDCs (Supplemental Fig. 4). This was also the case for CD86 where $CD19^+$ pDCs expressed higher levels of CD86 compared with $CD19^-$ pDCs. However, increased CD86 levels were consistently measured on $CD19^-$ pDCs from ABC and A′B strains compared with control mice and the B congenic strain (Fig. 6*C*). These results suggest that $CD19^+$ pDCs generally exhibit an activated phenotype relative to cDC and $CD19^-$ pDC under steady-state conditions, and that expression of the *Fcγ R* and *SLAM* intervals from *Nba2* can augment activation of both $CD19^-$ and $CD19^+$ pDCs.

Based on these results and previous studies that demonstrated the *SLAM* gene family was linked to spontaneous murine lupus (16, 17), we determined whether inheritance of the *Fcγ R* and *SLAM* intervals of *Nba2* differentially controlled protein expression of the *SLAM* receptors CD48, CD84, CD150, CD229, and Ly108. Results demonstrated expression differences that were restricted to ABC and A′B congenic strains where increased CD48 expression was

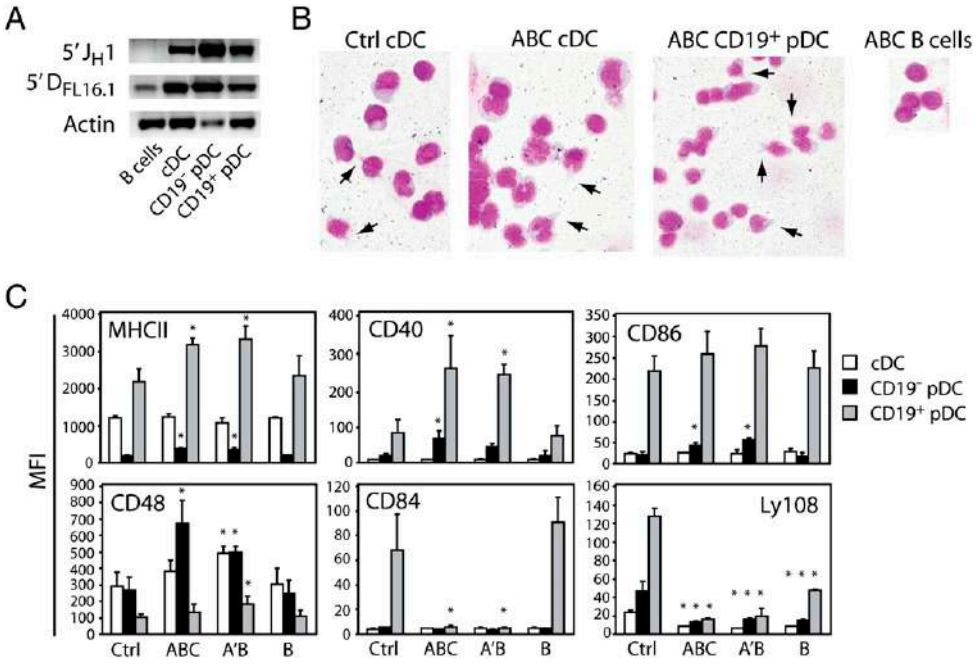

FIGURE 6. $CD19^+$ pDCs exhibit hallmark DC markers but have an altered activation phenotype that is associated with combined expression of *FcγR* and *SLAM* regions of *Nba2*. *A*, Ig gene rearrangement in sort-purified splenic B cell, cDC, $CD19^-$ pDC, and $CD19^+$ pDC populations from B6.*Nba2*-ABC congenic mice was determined by PCR analysis; transcripts for 5′ J_H1 and 5′ $D_{FL16.1}$ to determine D-J and V to D-J rearrangement, respectively, indicate Ig rearrangement in B cells where intron fragments have been deleted yet are retained in DC subsets. *B*, Cytospins of sort-purified cells were morphologically assessed by Giemsa staining. Arrows indicate dendrite formation. Images were taken at original magnification ×40. *C*, Spleen cells from 4-mo-old female mice were analyzed by FACS for the expression of indicated markers on cDCs, $CD19^-$ pDC, and $CD19^+$ pDCs using the same gating strategy described in Fig. 5. Results show the mean fluorescence intensity for each population. Statistical differences in the mean fluorescence intensity of a marker between congenic strains and B6 control mice are denoted by $*p < 0.05$. Data shown represent three independent experiments. Representative expression levels of all DC subset markers and *SLAM* receptors are shown in Supplemental Fig. 4.

measured on $CD19^-$ pDCs, reduced expression levels of CD84 were measured on $CD19^+$ pDCs, and reduced expression of Ly108 was measured on both $CD19^-$ and $CD19^+$ pDCs (Fig. 6*C*). Expression of *SLAM* receptor transcript levels in pDCs among congenic strains did not show a strong correlation with protein expression (Supplemental Fig. 5), suggesting that posttranscriptional regulation may contribute to differences in membrane receptor expression on pDCs.

Combined expression of FcγR *and* SLAM *intervals within* Nba2 *controls TLR9 sensitivity of pDCs to produce high amounts of cytokines that promote humoral immunity*

Recognition of pathogen-associated molecules by TLRs expressed on DCs triggers their activation that, in turn, results in the production of cytokines IL-6, IL-10, IL-12, and IFNα that promote humoral immunity by inducing growth and differentiation of B cells (44–47). Defective TLR signaling can inappropriately activate DCs, in particular pDCs, to secrete cytokines and has been implicated in facilitating the breakdown of tolerance [reviewed in (48)]. Therefore, we determined the cytokine-producing capacities of freshly isolated DCs in response to TLR signaling. Initial studies analyzed IL-10 and IL-6 secretion from total $CD11c^+$ DCs isolated from spleens of all mouse strains when cultured in vitro in the presence of the TLR4 stimulus LPS and the TLR9 ligand, CpG oligonucleotides, that mimics microbial DNA. Results demonstrated that significantly higher levels of IL-10 were produced by DCs from congenic ABC and A′B strains compared with control mice (Supplemental Fig. 6). These levels were similar to levels of IL-10 produced by DCs from NZB and (NZB × NZW)F_1 mice, indicating that the combined expression of *FcγR* and *SLAM* intervals within the *Nba2* locus is sufficient to control TLR hypersensitivity of DCs. To more thoroughly determine cytokine production, we analyzed the capacity of splenic DCs from control and congenic ABC mice to secrete IL-6, IL-10, IL-12, and IFNα in response to LPS, CpG, and the TLR7 stimulus R837 (imiquimod). Results demonstrated that although TLR stimulation induced IL-6 and IL-12 secretion, there were no differences measured between control and ABC congenic DCs (Fig. 7*A*). In contrast, DCs from congenic ABC mice produced significantly greater amounts of IL-10 and IFNα compared with control DCs where TLR9 stimulation induced the most cytokine. To determine whether increased levels of IL-10 and IFNα secretion by DCs from congenic ABC mice were the product of $CD19^-$ or $CD19^+$ pDCs, sort-purified pDC subsets were tested for cytokine secretion after TLR stimulation. Results demonstrated that both $CD19^-$ and $CD19^+$ pDCs from B6.*Nba2*-ABC mice produced significantly higher amounts of IL-10 compared with control pDCs, with the largest amount of IL-10 being produced in response to TLR9 stimulation (Fig. 7*B*). Similar results were measured for IFNα where both $CD19^-$ and $CD19^+$ pDCs from congenic mice produced the highest amount of cytokine after TLR9 stimulation. These data have at least two important findings. First, *Nba2* controls aberrant cytokine production by DCs, yet of the cytokines that influence B cell differentiation is limited to deregulation of IL-10 and IFNα. Second, although *Nba2* dramatically increases the frequency of $CD19^+$ pDCs (Fig. 5), the cytokine-producing capacities of both $CD19^-$ and $CD19^+$ pDCs are controlled by *Nba2*.

TLR9 stimulated pDCs can induce terminal B cell differentiation independent of T cell help and Ag (49, 50). Therefore, we determined the functional capacity of pDCs to license B cells to undergo PC differentiation. Sort-purified pDCs from spleens of congenic ABC, A′B, B, and C strains were cocultured with B6 control B cells in the presence of CpG. After 3 d, the frequency of total Ig-secreting PCs was quantified by ELISPOT. Coculture of

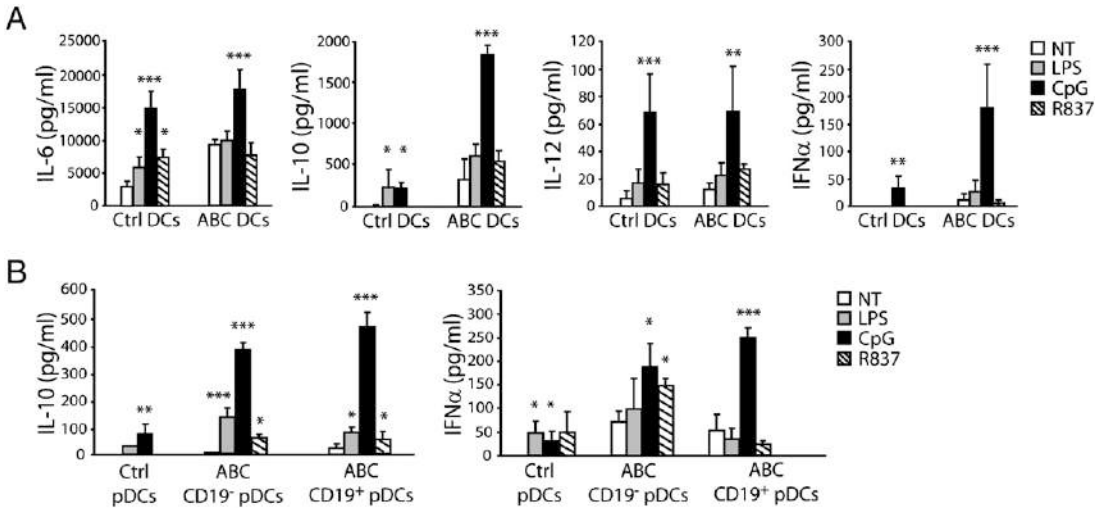

FIGURE 7. The *Nba2* locus controls TLR hypersensitivity of DCs to produce proinflammatory cytokines. *A*, Total CD11c$^+$ DCs were sort-purified from spleens of 4-mo-old B6.*Nba2*-ABC and B6 control mice, and were cultured 24 h in the absence (no treatment [NT]) or presence of 100 ng/ml LPS, 10 μg/ml CpG, and 10 μg/ml R837. Supernatants were collected and the amount of cytokine was determined by ELISA. Statistical differences between TLR-stimulated groups and NT are indicated by $*p < 0.05$, $**p < 0.01$, and $***p < 0.001$. *B*, Using identical culture conditions, levels of IL-10 and IFNα were determined from purified total pDCs or CD19$^-$ and CD19$^+$ pDCs. Data are expressed as the mean ± SEM from 6–9 mice per group. NT, no treatment.

pDCs and B cells from B6 control mice served as a normal control. Results demonstrated that B cells cultured alone, with CpG, or with the control GpC oligonucleotide produced only small numbers of PCs, indicating that by itself TLR9 signaling on B cells minimally supports B cell differentiation (Fig. 8*A*). Parallel cultures containing only pDCs served as negative controls. Significant numbers of PCs were measured when B cells and pDCs from control and congenic ABC mice were cocultured in the presence of CpG, with the highest number of PCs generated from groups containing congenic ABC pDCs. This response was specific for TLR9 activation because the addition of control GpC did not induce PC differentiation. Furthermore, the ability of pDCs to drive PC differentiation was dependent, in part, by secretion of IL-10 and IFNα as demonstrated by reduced PC numbers when neutralizing mAbs to these cytokines were added to cocultures (Fig. 8*B*). Significantly high numbers of PCs were generated in cocultures containing pDCs from congenic ABC, A′B, and B strains, suggesting that the *Nba2*-derived *SLAM* interval alone is sufficient for promoting heightened Ab production in a TLR9-dependent manner. Analysis of cocultures containing pDCs from congenic C mice, which do not express the *SLAM* interval from *Nba2*, produced significantly fewer PCs.

Discussion

We have previously shown that when the entire 40 Mb *Nba2* locus is expressed on the nonautoimmune B6 background, female congenic animals produce elevated levels of serum ANA, increased B cell proliferation, increased type I IFN, and severe GN when crossed with NZW mice (7, 21). In this study, we analyzed subcongenic strains to determine the gene clusters within *Nba2* that contribute to these autoimmune traits. The analysis of five subcongenic strains revealed that combined expression of the *Fcγ R* and *SLAM* intervals (A′B strain), spanning ~6.8 Mb within the central region of *Nba2*, is sufficient to reproduce the autoimmune phenotype of the parental congenic strain. Further analyses of subcongenic strains that independently express the *Fcγ R* interval (A strain) from the *SLAM* interval (B, BC, and C strains) demonstrated that each of these gene clusters, alone, could not drive autoantibody production. Interestingly, these studies also revealed that genes located proximal to the *Fcγ R* interval as well as genes located distal to the *SLAM* interval do not contribute to ANA production, even if allowed to epistatically interact with susceptibility genes derived from NZW mice (A, C strains × NZW). This suggests that the lupus susceptibility genes located within the *Ifi* interval do not mediate a loss in B cell tolerance and autoantibody production. However, genes of the *Ifi200* family could indirectly contribute to the autoimmune phenotype by inhibiting p53- and E2F1-mediated proapoptotic functions as has previously been suggested (22, 51). Furthermore, data presented in Supplemental Fig. 5 suggests that the *SLAM* genes, *CD48*, *CD84*, and *CD229* could be epistatically regulated by genes expressed within the *Ifi* interval.

The contribution of the *Fcγ R* interval in mediating autoantibody production appears to be through deregulation of B cell homeostasis by reducing FcγRIIb expression on terminally differentiating B cells, resulting in impaired apoptosis. Human SLE genome screens have consistently identified significant linkage at the 1q23 locus where *Fcγ R* genes reside (52–54), suggesting that one or more of the Fc receptor genes contributes to human SLE. This hypothesis is supported in murine experimental systems that have demonstrated a deficiency in the *Fcγ RIIb* gene leads to increased ANA IgG (12, 55). Although the most likely candidates in the A' region of *Nba2* are the *Fcγ R* genes, it is possible that other genes play a role in B cell differentiation and survival. Fine mapping the 122 genes that span the A' region by generating additional subcongenic lines that contain narrower intervals will facilitate identifying candidate genes.

How inheritance of the *Nba2* B region, containing the *SLAM* interval, contributes to the disease process is less clear. Genomic characterization of B6.*Sle1b* congenic mice has demonstrated extensive polymorphisms in exons encoding the extracellular domains of several *SLAM* receptors, including CD48, CD84, and Ly108 (16). Although it is not understood how these polymorphic variants mediate the *Sle1b* autoimmune phenotype, differential receptor expression on both T and B lymphocytes may influence cellular activation and survival. Increased levels of the *ly108-1* isoform by B cells from B6.*Sle1b* mice are associated with increased survival and impaired deletion of autoreactive B cells (17). Interestingly, we demonstrated that CD48, CD84, and Ly108 were differentially expressed on DCs from congenic ABC and A′B strains compared with the congenic B strain and control mice.

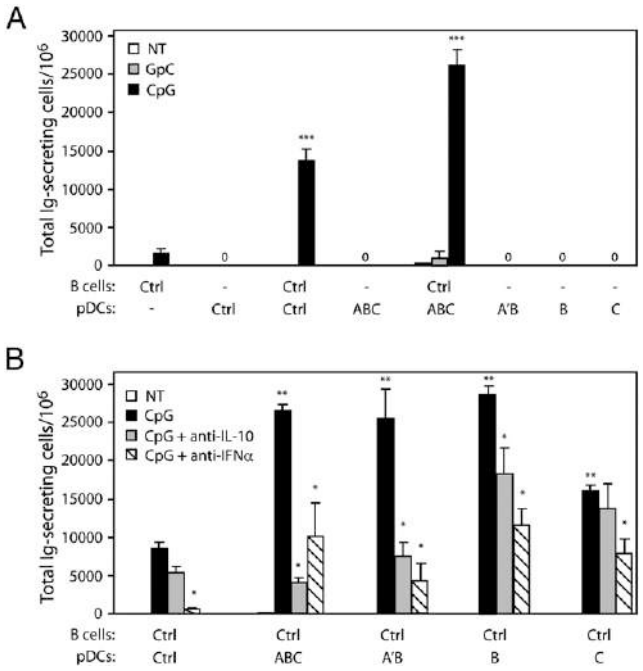

FIGURE 8. Combined expression of *Fc*γ*R* and *SLAM* intervals control TLR hypersensitivity of pDCs to promote the generation of Ab-secreting cells. *A*, Purified B220$^+$CD11c^{int} pDCs from spleens of congenic ABC, A′B, B, and C strains as well as B6 control mice were cultured with an equal number (1×10^4) of purified control B cells in medium alone (NT), with 10 μg/ml CpG, or with 10 μg/ml nonstimulatory GpC oligonucleotide. B cells and pDCs cultured alone served as negative controls. After 72 h, the number of total Ig-secreting cells was determined by ELISPOT. Statistical differences between CpG stimulated groups and control GpC groups are indicated by $***p < 0.001$. *B*, B cells and pDCs were also cocultured in the presence of neutralizing mAb specific for IL-10 (5 μg/ml) and IFNα (10 μg/ml) throughout the 72 h, followed by ELISPOT. Statistical differences between CpG-stimulated groups containing pDCs from congenic strains and control mice are indicated as $**p < 0.01$. CpG-stimulated groups with IL-10 and IFNα neutralizing mAb that had statistically fewer Ab-secreting cells compared with CpG alone are designated $*p < 0.05$. Data are expressed as the mean ± SEM from three replicates per group that represent two independent experiments. NT, no treatment.

These findings suggest that, within *Nba2*, altered expression of SLAM receptors is controlled by both *Fc*γ*R* and *SLAM* intervals. Exactly what functional impact altered SLAM receptor expression has on DCs will require more study, but we hypothesize that SLAM receptors on DCs provide regulatory cues to their counter-receptors on T and B cells during Ag presentation that direct lymphocyte proliferation and/or differentiation. Consistent with this hypothesis, recent studies have suggested a potential role for CD150 in human DC activation by influencing the production of IL-6 and IL-12 (56, 57). Thus, it is possible that susceptibility genes within the *SLAM* family or other genes, such as *Apsc* (serum amyloid P) and *Crp* that are also located within the B region of *Nba2*, increase cytokine production by DCs that contributes to the autoimmune phenotype.

In addition to differences in SLAM receptor expression, analysis of DCs among the congenic strains revealed that the number and phenotype of pDCs were controlled by both *Fc*γ*R* and *SLAM* intervals. Significantly increased numbers of pDCs that were vastly CD19$^+$ were found in congenic A′B mice that reproduced those found in the congenic ABC parental strain, yet were only modestly increased in congenic B mice. These findings suggest that it is the combination of the *Fc*γ*R* and *SLAM* intervals that control the frequency of CD19$^+$ pDCs. Interestingly, numbers of CD19$^+$ pDCs were similarly elevated in congenic BC and C strains compared with B6 control mice, further suggesting that genes within the C region of *Nba2* influence the expansion of CD19$^+$ pDCs. Mellor and coworkers (58) first identified CD19$^+$ DCs as a rare subset of splenic DCs in healthy mice that could suppress T cell proliferation in a manner dependent on expression of the enzyme IDO by CD19$^+$ DCs. Mellor and colleagues (33) subsequently demonstrated that splenic CD19$^+$ DCs acquired potent IDO-dependent T cell suppressor activity after in vivo administration of CpG and that IFNα signaling was essential for IDO expression. Limited phenotypic analysis of these CD19$^+$ DCs makes it unknown whether this population is identical to CD19$^+$ pDCs found in congenic *Nba2* strains. However, recent studies have demonstrated that IDO-expressing pDCs directly activated natural T regulatory cells for potent suppressor activity (59), and promoted the generation of inducible T regulatory cells (60). Current studies are underway to determine whether CD19$^+$ pDCs from congenic *Nba2* mice express IDO and are able to suppress T cell proliferation.

Consistent with increased numbers of pDCs from congenic ABC and A′B strains, were increased CD40, CD86, and Siglec-H expression levels compared with cDCs, suggesting that combined expression of *Fc*γ*R* and *SLAM* intervals may trigger heightened steady-state activation levels of pDCs to produce increased proinflammatory cytokines. Analysis of TLR9-stimulated DCs from congenic ABC mice demonstrated that only IL-10 and IFNα levels were significantly increased compared with control DCs, and moreover, were mainly produced by CD19$^-$ and CD19$^+$ pDCs. IL-10 and IFNα have been associated with proinflammatory properties during an immune response and to be deregulated in autoimmunity. Increased levels of serum IL-10 have been measured in SLE patients and correlate with ANA production and disease activity (61, 62). Furthermore, in both lupus-prone mice (63) and SLE patients (64), administration of a neutralizing IL-10 mAb-reduced cutaneous lesions and rheumatologic symptoms, indicating that IL-10 is a major player in autoantibody production and mediating tissue damage. How IL-10 specifically functions in the disease process is unclear, but the capacity of IL-10 to promote B cell proliferation and differentiation to PCs strongly suggests it alters the B cell compartment by increasing the generation of ANA-producing PCs (65, 66). Similarly, IFNα is also believed to be an important proinflammatory cytokine in the generation of autoreactive PCs (44), with pDCs being the primary source of IFNα (67–69). Analysis of pDCs from congenic strains demonstrated that the *SLAM* interval within *Nba2* licenses pDCs to drive PC differentiation in an IL-10- and IFNα-dependent manner.

In conclusion, we have narrowed down the contribution of the *Nba2* locus to murine lupus susceptibility to a central region (169.1–175.9 Mb) that contains the *Fc*γ*R* and *SLAM* intervals. The combined expression of both intervals influences the homeostasis of GC B cells and PCs, and promotes PC differentiation through deregulated activation of pDCs. Importantly, our findings advance our understanding of how susceptibility genes within the telomeric region of chromosome 1 control autoantibody production and indicate that the *Fc*γ*R* and *SLAM* intervals each control different immune pathways, yet are both required for the development of ANA and renal disease.

Acknowledgments

We thank Joanne Lannigan and Michael Solga of the University of Virginia Flow Cytometry Core, and Katherine Menze, Heather Steele, and Chinonye Ihekweazu of the UCHSC for expert technical assistance.

Disclosures

The authors have no financial conflicts of interest.

References

1. Wakeland, E. K., K. Liu, R. R. Graham, and T. W. Behrens. 2001. Delineating the genetic basis of systemic lupus erythematosus. *Immunity* 15: 397–408.
2. Pisetsky, D. S. 2000. Anti-DNA and autoantibodies. *Curr. Opin. Rheumatol.* 12: 364–368.
3. Chan, O. T., M. P. Madaio, and M. J. Shlomchik. 1999. The central and multiple roles of B cells in lupus pathogenesis. *Immunol. Rev.* 169: 107–121.
4. Wakeland, E. K., A. E. Wandstrat, K. Liu, and L. Morel. 1999. Genetic dissection of systemic lupus erythematosus. *Curr. Opin. Immunol.* 11: 701–707.
5. Morel, L., Y. Yu, K. R. Blenman, R. A. Caldwell, and E. K. Wakeland. 1996. Production of congenic mouse strains carrying genomic intervals containing SLE-susceptibility genes derived from the SLE-prone NZM2410 strain. *Mamm. Genome* 7: 335–339.
6. Rozzo, S. J., T. J. Vyse, C. G. Drake, and B. L. Kotzin. 1996. Effect of genetic background on the contribution of New Zealand black loci to autoimmune lupus nephritis. *Proc. Natl. Acad. Sci. U.S.A.* 93: 15164–15168.
7. Rozzo, S. J., J. D. Allard, D. Choubey, T. J. Vyse, S. Izui, G. Peltz, and B. L. Kotzin. 2001. Evidence for an interferon-inducible gene, Ifi202, in the susceptibility to systemic lupus. *Immunity* 15: 435–443.
8. Stohl, W., D. Xu, T. E. Metzger, K. S. Kim, L. Morel, and B. L. Kotzin. 2004. Dichotomous effects of complete versus partial class II major histocompatibility complex deficiency on circulating autoantibody levels in autoimmune-prone mice. *Arthritis Rheum.* 50: 2227–2239.
9. Mohan, C., E. Alas, L. Morel, P. Yang, and E. K. Wakeland. 1998. Genetic dissection of SLE pathogenesis. Sle1 on murine chromosome 1 leads to a selective loss of tolerance to H2A/H2B/DNA subnucleosomes. *J. Clin. Invest.* 101: 1362–1372.
10. Morel, L., C. Mohan, Y. Yu, B. P. Croker, N. Tian, A. Deng, and E. K. Wakeland. 1997. Functional dissection of systemic lupus erythematosus using congenic mouse strains. *J. Immunol.* 158: 6019–6028.
11. Gubbels, M. R., T. N. Jørgensen, T. E. Metzger, K. Menze, H. Steele, S. A. Flannery, S. J. Rozzo, and B. L. Kotzin. 2005. Effects of MHC and gender on lupus-like autoimmunity in Nba2 congenic mice. *J. Immunol.* 175: 6190–6196.
12. Bolland, S., Y. S. Yim, K. Tus, E. K. Wakeland, and J. V. Ravetch. 2002. Genetic modifiers of systemic lupus erythematosus in FcgammaRIIB($^{-/-}$) mice. *J. Exp. Med.* 195: 1167–1174.
13. Rahman, Z. S., and T. Manser. 2005. Failed up-regulation of the inhibitory IgG Fc receptor Fc γ RIIB on germinal center B cells in autoimmune-prone mice is not associated with deletion polymorphisms in the promoter region of the Fc γ RIIB gene. *J. Immunol.* 175: 1440–1449.
14. Jiang, Y., S. Hirose, R. Sanokawa-Akakura, M. Abe, X. Mi, N. Li, Y. Miura, J. Shirai, D. Zhang, Y. Hamano, and T. Shirai. 1999. Genetically determined aberrant down-regulation of FcgammaRIIB1 in germinal center B cells associated with hyper-IgG and IgG autoantibodies in murine systemic lupus erythematosus. *Int. Immunol.* 11: 1685–1691.
15. Pritchard, N. R., A. J. Cutler, S. Uribe, S. J. Chadban, B. J. Morley, and K. G. Smith. 2000. Autoimmune-prone mice share a promoter haplotype associated with reduced expression and function of the Fc receptor FcgammaRII. *Curr. Biol.* 10: 227–230.
16. Wandstrat, A. E., C. Nguyen, N. Limaye, A. Y. Chan, S. Subramanian, X. H. Tian, Y. S. Yim, A. Pertsemlidis, H. R. Garner, Jr., L. Morel, and E. K. Wakeland. 2004. Association of extensive polymorphisms in the SLAM/CD2 gene cluster with murine lupus. *Immunity* 21: 769–780.
17. Kumar, K. R., L. Li, M. Yan, M. Bhaskarabhatla, A. B. Mobley, C. Nguyen, J. M. Mooney, J. D. Schatzle, E. K. Wakeland, and C. Mohan. 2006. Regulation of B cell tolerance by the lupus susceptibility gene Ly108. *Science* 312: 1665–1669.
18. Vyse, T. J., S. J. Rozzo, C. G. Drake, S. Izui, and B. L. Kotzin. 1997. Control of multiple autoantibodies linked with a lupus nephritis susceptibility locus in New Zealand black mice. *J. Immunol.* 158: 5566–5574.
19. Hardy, R. R., C. E. Carmack, S. A. Shinton, J. D. Kemp, and K. Hayakawa. 1991. Resolution and characterization of pro-B and pre-pro-B cell stages in normal mouse bone marrow. *J. Exp. Med.* 173: 1213–1225.
20. Erickson, L. D., B. G. Durell, L. A. Vogel, B. P. O'Connor, M. Cascalho, T. Yasui, H. Kikutani, and R. J. Noelle. 2002. Short-circuiting long-lived humoral immunity by the heightened engagement of CD40. *J. Clin. Invest.* 109: 613–620.
21. Jørgensen, T. N., E. Roper, J. M. Thurman, P. Marrack, and B. L. Kotzin. 2007. Type I interferon signaling is involved in the spontaneous development of lupus-like disease in B6.Nba2 and (B6.Nba2 x NZW)F(1) mice. *Genes Immun.* 8: 653–662.
22. Xin, H., S. D'Souza, T. N. Jørgensen, A. T. Vaughan, P. Lengyel, B. L. Kotzin, and D. Choubey. 2006. Increased expression of Ifi202, an IFN-activatable gene, in B6.Nba2 lupus susceptible mice inhibits p53-mediated apoptosis. *J. Immunol.* 176: 5863–5870.
23. Ravetch, J. V., and S. Bolland. 2001. IgG Fc receptors. *Annu. Rev. Immunol.* 19: 275–290.
24. Pearse, R. N., T. Kawabe, S. Bolland, R. Guinamard, T. Kurosaki, and J. V. Ravetch. 1999. SHIP recruitment attenuates Fc γ RIIB-induced B cell apoptosis. *Immunity* 10: 753–760.
25. Tzeng, S. J., S. Bolland, K. Inabe, T. Kurosaki, and S. K. Pierce. 2005. The B cell inhibitory Fc receptor triggers apoptosis by a novel c-Abl family kinase-dependent pathway. *J. Biol. Chem.* 280: 35247–35254.
26. Xiang, Z., A. J. Cutler, R. J. Brownlie, K. Fairfax, K. E. Lawlor, E. Severinson, E. U. Walker, R. A. Manz, D. M. Tarlinton, and K. G. Smith. 2007. FcgammaRIIb controls bone marrow plasma cell persistence and apoptosis. *Nat. Immunol.* 8: 419–429.
27. Laszlo, G., K. S. Hathcock, H. B. Dickler, and R. J. Hodes. 1993. Characterization of a novel cell-surface molecule expressed on subpopulations of activated T and B cells. *J. Immunol.* 150: 5252–5262.
28. Calame, K. L. 2001. Plasma cells: finding new light at the end of B cell development. *Nat. Immunol.* 2: 1103–1108.
29. Banchereau, J., F. Briere, C. Caux, J. Davoust, S. Lebecque, Y. J. Liu, B. Pulendran, and K. Palucka. 2000. Immunobiology of dendritic cells. *Annu. Rev. Immunol.* 18: 767–811.
30. Steinman, R. M., D. Hawiger, and M. C. Nussenzweig. 2003. Tolerogenic dendritic cells. *Annu. Rev. Immunol.* 21: 685–711.
31. Jørgensen, T. N., J. Thurman, S. Izui, M. T. Falta, T. E. Metzger, S. A. Flannery, J. Kappler, P. Marrack, and B. L. Kotzin. 2006. Genetic susceptibility to polyI:C-induced IFNalpha/β-dependent accelerated disease in lupus-prone mice. *Genes Immun.* 7: 555–567.
32. Baban, B., A. M. Hansen, P. R. Chandler, A. Manlapat, A. Bingaman, D. J. Kahler, D. H. Munn, and A. L. Mellor. 2005. A minor population of splenic dendritic cells expressing CD19 mediates IDO-dependent T cell suppression via type I IFN signaling following B7 ligation. *Int. Immunol.* 17: 909–919.
33. Mellor, A. L., B. Baban, P. R. Chandler, A. Manlapat, D. J. Kahler, and D. H. Munn. 2005. Cutting edge: CpG oligonucleotides induce splenic CD19+ dendritic cells to acquire potent indoleamine 2,3-dioxygenase-dependent T cell regulatory functions via IFN Type 1 signaling. *J. Immunol.* 175: 5601–5605.
34. Blasius, A. L., M. Cella, J. Maldonado, T. Takai, and M. Colonna. 2006. Siglec-H is an IPC-specific receptor that modulates type I IFN secretion through DAP12. *Blood* 107: 2474–2476.
35. Zhang, J., A. Raper, N. Sugita, R. Hingorani, M. Salio, M. J. Palmowski, V. Cerundolo, and P. R. Crocker. 2006. Characterization of Siglec-H as a novel endocytic receptor expressed on murine plasmacytoid dendritic cell precursors. *Blood* 107: 3600–3608.
36. Atencio, S., H. Amano, S. Izui, and B. L. Kotzin. 2004. Separation of the New Zealand Black genetic contribution to lupus from New Zealand Black determined expansions of marginal zone B and B1a cells. *J. Immunol.* 172: 4159–4166.
37. Corcoran, L., I. Ferrero, D. Vremec, K. Lucas, J. Waithman, M. O'Keeffe, L. Wu, A. Wilson, and K. Shortman. 2003. The lymphoid past of mouse plasmacytoid cells and thymic dendritic cells. *J. Immunol.* 170: 4926–4932.
38. Pelayo, R., J. Hirose, J. Huang, K. P. Garrett, A. Delogu, M. Busslinger, and P. W. Kincade. 2005. Derivation of 2 categories of plasmacytoid dendritic cells in murine bone marrow. *Blood* 105: 4407–4415.
39. Shigematsu, H., B. Reizis, H. Iwasaki, S. Mizuno, D. Hu, D. Traver, P. Leder, N. Sakaguchi, and K. Akashi. 2004. Plasmacytoid dendritic cells activate lymphoid-specific genetic programs irrespective of their cellular origin. *Immunity* 21: 43–53.
40. Chan, C. W., E. Crafton, H. N. Fan, J. Flook, K. Yoshimura, M. Skarica, D. Brockstedt, T. W. Dubensky, M. F. Stins, L. L. Lanier, et al. 2006. Interferon-producing killer dendritic cells provide a link between innate and adaptive immunity. *Nat. Med.* 12: 207–213.
41. Sato, K., and S. Fujita. 2007. Dendritic cells: nature and classification. *Allergol. Int.* 56: 183–191.
42. Wu, L., and Y. J. Liu. 2007. Development of dendritic-cell lineages. *Immunity* 26: 741–750.
43. Blasius, A. L., W. Barchet, M. Cella, and M. Colonna. 2007. Development and function of murine B220+CD11c+NK1.1+ cells identify them as a subset of NK cells. *J. Exp. Med.* 204: 2561–2568.
44. Jego, G., A. K. Palucka, J. P. Blanck, C. Chalouni, V. Pascual, and J. Banchereau. 2003. Plasmacytoid dendritic cells induce plasma cell differentiation through type I interferon and interleukin 6. *Immunity* 19: 225–234.
45. Fayette, J., I. Durand, J. M. Bridon, C. Arpin, B. Dubois, C. Caux, Y. J. Liu, J. Banchereau, and F. Brière. 1998. Dendritic cells enhance the differentiation of naïve B cells into plasma cells in vitro. *Scand. J. Immunol.* 48: 563–570.
46. Dubois, B., C. Massacrier, B. Vanbervliet, J. Fayette, F. Brière, J. Banchereau, and C. Caux. 1998. Critical role of IL-12 in dendritic cell-induced differentiation of naive B lymphocytes. *J. Immunol.* 161: 2223–2231.
47. Hochrein, H., K. Shortman, D. Vremec, B. Scott, P. Hertzog, and M. O'Keeffe. 2001. Differential production of IL-12, IFN-α, and IFN-γ by mouse dendritic cell subsets. *J. Immunol.* 166: 5448–5455.
48. Marshak-Rothstein, A. 2006. Toll-like receptors in systemic autoimmune disease. *Nat. Rev. Immunol.* 6: 823–835.
49. Poeck, H., M. Wagner, J. Battiany, S. Rothenfusser, D. Wellisch, V. Hornung, B. Jahrsdorfer, T. Giese, S. Endres, and G. Hartmann. 2004. Plasmacytoid dendritic cells, antigen, and CpG-C license human B cells for plasma cell differentiation and immunoglobulin production in the absence of T-cell help. *Blood* 103: 3058–3064.
50. Bekeredjian-Ding, I. B., M. Wagner, V. Hornung, T. Giese, M. Schnurr, S. Endres, and G. Hartmann. 2005. Plasmacytoid dendritic cells control TLR7 sensitivity of naive B cells via type I IFN. [Published erratum appears in 2005 *J. Immunol.* 174:5884.] *J. Immunol.* 174: 4043–4050.
51. Panchanathan, R., H. Xin, and D. Choubey. 2008. Disruption of mutually negative regulatory feedback loop between interferon-inducible p202 protein and the E2F family of transcription factors in lupus-prone mice. *J. Immunol.* 180: 5927–5934.
52. Tsao, B. P., R. M. Cantor, K. C. Kalunian, C. J. Chen, H. Badsha, R. Singh, D. J. Wallace, R. C. Kitridou, S. L. Chen, N. Shen, et al. 1997. Evidence for linkage of a candidate chromosome 1 region to human systemic lupus erythematosus. *J. Clin. Invest.* 99: 725–731.

53. Moser, K. L., B. R. Neas, J. E. Salmon, H. Yu, C. Gray-McGuire, N. Asundi, G. R. Bruner, J. Fox, J. Kelly, S. Henshall, et al. 1998. Genome scan of human systemic lupus erythematosus: evidence for linkage on chromosome 1q in African-American pedigrees. *Proc. Natl. Acad. Sci. U.S.A.* 95: 14869–14874.
54. Shai, R., F. P. Quismorio, Jr., L. Li, O. J. Kwon, J. Morrison, D. J. Wallace, C. M. Neuwelt, C. Brautbar, W. J. Gauderman, and C. O. Jacob. 1999. Genome-wide screen for systemic lupus erythematosus susceptibility genes in multiplex families. *Hum. Mol. Genet.* 8: 639–644.
55. Takai, T., M. Ono, M. Hikida, H. Ohmori, and J. V. Ravetch. 1996. Augmented humoral and anaphylactic responses in Fc γ RII-deficient mice. *Nature* 379: 346–349.
56. Bleharski, J. R., K. R. Niazi, P. A. Sieling, G. Cheng, and R. L. Modlin. 2001. Signaling lymphocytic activation molecule is expressed on CD40 ligand-activated dendritic cells and directly augments production of inflammatory cytokines. *J. Immunol.* 167: 3174–3181.
57. Réthi, B., P. Gogolák, I. Szatmari, A. Veres, E. Erdôs, L. Nagy, E. Rajnavölgyi, C. Terhorst, and A. Lányi. 2006. SLAM/SLAM interactions inhibit CD40-induced production of inflammatory cytokines in monocyte-derived dendritic cells. *Blood* 107: 2821–2829.
58. Mellor, A. L., P. Chandler, B. Baban, A. M. Hansen, B. Marshall, J. Pihkala, H. Waldmann, S. Cobbold, E. Adams, and D. H. Munn. 2004. Specific subsets of murine dendritic cells acquire potent T cell regulatory functions following CTLA4-mediated induction of indoleamine 2,3 dioxygenase. *Int. Immunol.* 16: 1391–1401.
59. Sharma, M. D., B. Baban, P. Chandler, D. Y. Hou, N. Singh, H. Yagita, M. Azuma, B. R. Blazar, A. L. Mellor, and D. H. Munn. 2007. Plasmacytoid dendritic cells from mouse tumor-draining lymph nodes directly activate mature Tregs via indoleamine 2,3-dioxygenase. *J. Clin. Invest.* 117: 2570–2582.
60. Chen, W., X. Liang, A. J. Peterson, D. H. Munn, and B. R. Blazar. 2008. The indoleamine 2,3-dioxygenase pathway is essential for human plasmacytoid dendritic cell-induced adaptive T regulatory cell generation. *J. Immunol.* 181: 5396–5404.
61. Park, Y. B., S. K. Lee, D. S. Kim, J. Lee, C. H. Lee, and C. H. Song. 1998. Elevated interleukin-10 levels correlated with disease activity in systemic lupus erythematosus. *Clin. Exp. Rheumatol.* 16: 283–288.
62. Chun, H. Y., J. W. Chung, H. A. Kim, J. M. Yun, J. Y. Jeon, Y. M. Ye, S. H. Kim, H. S. Park, and C. H. Suh. 2007. Cytokine IL-6 and IL-10 as biomarkers in systemic lupus erythematosus. *J. Clin. Immunol.* 27: 461–466.
63. Ishida, H., T. Muchamuel, S. Sakaguchi, S. Andrade, S. Menon, and M. Howard. 1994. Continuous administration of anti-interleukin 10 antibodies delays onset of autoimmunity in NZB/W F1 mice. *J. Exp. Med.* 179: 305–310.
64. Llorente, L., Y. Richaud-Patin, C. García-Padilla, E. Claret, J. Jakez-Ocampo, M. H. Cardiel, J. Alcocer-Varela, L. Grangeot-Keros, D. Alarcón-Segovia, J. Wijdenes, et al. 2000. Clinical and biologic effects of anti-interleukin-10 monoclonal antibody administration in systemic lupus erythematosus. *Arthritis Rheum.* 43: 1790–1800.
65. Rousset, F., E. Garcia, T. Defrance, C. Peronne, N. Vezzio, D. H. Hsu, R. Kastelein, K. W. Moore, and J. Banchereau. 1992. Interleukin 10 is a potent growth and differentiation factor for activated human B lymphocytes. *Proc. Natl. Acad. Sci. U.S.A.* 89: 1890–1893.
66. Llorente, L., W. Zou, Y. Levy, Y. Richaud-Patin, J. Wijdenes, J. Alcocer-Varela, B. Morel-Fourrier, J. C. Brouet, D. Alarcon-Segovia, P. Galanaud, and D. Emilie. 1995. Role of interleukin 10 in the B lymphocyte hyperactivity and autoantibody production of human systemic lupus erythematosus. *J. Exp. Med.* 181: 839–844.
67. Cella, M., D. Jarrossay, F. Facchetti, O. Alebardi, H. Nakajima, A. Lanzavecchia, and M. Colonna. 1999. Plasmacytoid monocytes migrate to inflamed lymph nodes and produce large amounts of type I interferon. *Nat. Med.* 5: 919–923.
68. Siegal, F. P., N. Kadowaki, M. Shodell, P. A. Fitzgerald-Bocarsly, K. Shah, S. Ho, S. Antonenko, and Y. J. Liu. 1999. The nature of the principal type 1 interferon-producing cells in human blood. *Science* 284: 1835–1837.